Self-Induced Backaction Optical Pulling Force

Tongtong Zhu,[1,2] Yongyin Cao,[1] Lin Wang,[1] Zhongquan Nie,[3] Tun Cao,[4] Fangkui Sun,[1] Zehui Jiang,[1] Manuel Nieto-Vesperinas,[5] Yongmin Liu,[6,*] Cheng-Wei Qiu,[2,†] and Weiqiang Ding[1,‡]

[1]*Department of Physics, Harbin Institute of Technology, Harbin 150001, China*

[2]*Department of Electrical and Computer Engineering, National University of Singapore, 4 Engineering Drive 3, Singapore 117583, Singapore*

[3]*Key Lab of Advanced Transducers and Intelligent Control System, Ministry of Education and Shanxi Province, College of Physics and Optoelectronics, Taiyuan University of Technology, Taiyuan 030024, China*

[4]*Department of Biomedical Engineering, Dalian University of Technology, Dalian 116024, China*

[5]*Instituto de Ciencia de Materiales de Madrid, Consejo Superior de Investigaciones Científicas, Campus de Cantoblanco, Madrid 28049, Spain*

[6]*Departments of Mechanical and Industrial Engineering and Electrical and Computer Engineering, Northeastern University, Boston, Massachusetts 02115, USA*

(Received 11 November 2017; published 21 March 2018; corrected 23 March 2018)

We achieve long-range and continuous optical pulling in a periodic photonic crystal background, which supports a unique Bloch mode with the self-collimation effect. Most interestingly, the pulling force reported here is mainly contributed by the *intensity gradient force* originating from the self-induced backaction of the object to the self-collimation mode. This force is sharply distinguished from the widely held conception of optical tractor beams based on the scattering force. Also, this pulling force is insensitive to the angle of incidence and can pull multiple objects simultaneously.

DOI: 10.1103/PhysRevLett.120.123901

Since the pioneering work of Ashkin [1–3], the concepts and techniques of matter trapping and manipulation by an optical force have experienced impressive progress in the past decades [4–7]. Optical tweezers have become an indispensable tool in various disciplines, including biology [8–10], optics [11–13], and condensed matter [14], as well as quantum physics [15]. In traditional optical trapping, however, it is extremely challenging to scale down below 100 nm due to both the diffraction-limited focusing of light and the r^{-3} decaying law of the optical force with the radius r of small particles. Under these circumstances, by setting the trapping operation inside a nanocavity, the self-induced backaction optical trapping was proposed in nanoapertures [16–22], which can trap objects of tens of nanometers, or even smaller, thanks to the active feedback of the trapping objects to the trapping system.

Despite its power in nanometric trapping, the self-induced backaction method has not been explored in long-range optical pulling (or as optical tractor beams), because it enhances the intensity *gradient* component of the trapping force in a nanoaperture, while a tractor beam relies on the *scattering* component in a translation-invariant structure. A tractor beam, initially proposed in acoustics by Marston *et al.* [23–25], is an intensity gradientless beam along the propagation direction, which can transport objects towards the source over a long distance rather than push them away. The counterintuitive optical pulling [26–28] raises increasing attention due to its sophisticated underlying physics and potential applications [26–48].

In the extensive studies up to now, except for the photophoretic forces [49,50], all optical pulling forces have been regarded as optical scattering forces, like in the schemes of structured light beams [26–33,40], exotic media [41,42,51,52], inhomogeneous background media [38,53], and guiding mode scattering [34,44,54].

In this Letter, we propose a novel approach based on the self-induced backaction-generated gradient force that achieves long-range optical pulling in a periodic photonic structure, namely, in a photonic crystal (PC) [55,56]. Interestingly, the pulling force arising in the PC *is not* predominantly contributed by the scattering force as reported before but induced by the intensity gradient force generated by the dynamic interaction of the object with the self-collimation (SC) mode of the PC [57–59]. The SC mode is a unique kind of Bloch mode with a finite transversal size that can propagate infinitely long without diffraction. Hence, our results are sharply distinct to the widely held conception that the optical pulling force should be a scattering force, and shed new insightful concepts concerning the optical force and momentum physics and technologies.

To illustrate the underlining physics, we address a two-dimensional PC structure with a square lattice as illustrated in Fig. 1. Figure 1(a) shows the outline of the entire configuration. The SC mode is excited by a Gaussian beam at an angle of incidence θ_{in} and propagates along the $+x$

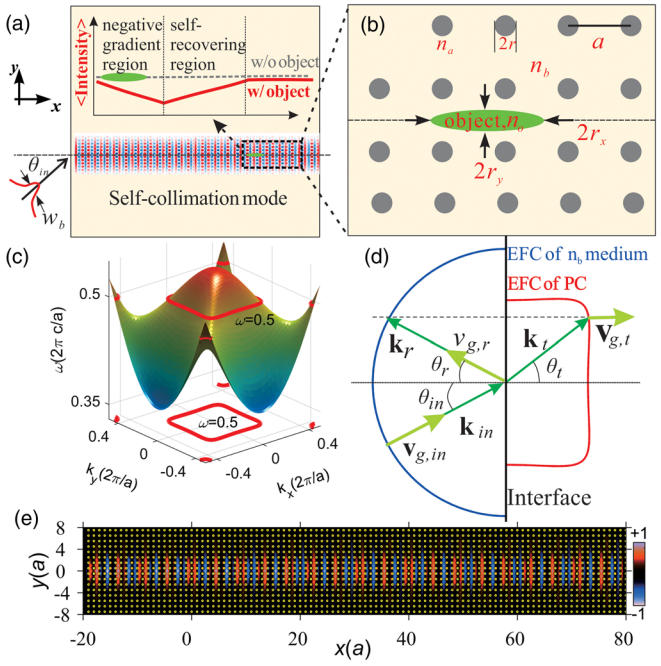

FIG. 1. (a) Schematic of the optical pulling force enabled by the SC mode in a PC. The upper inset shows the intensity envelopes across the SC mode axis without (gray dashed line) and with (red solid line) the object. The green ellipse shows the object. (b) Detailed structure of the square lattice (lattice constant a) PC and the object. The parameters are $n_a = 3.4$, $n_b = 1.33$, $n_o = 1.5$, $r = 0.1a$, and semiaxes of r_x and r_y. (c) The second band in the reduced Brillion zone for the TM mode (electric field perpendicular to the xy plane). For $\omega = 0.5(2\pi c/a)$, the equifrequency contour is square, which is the distinguishing characteristic of the SC mode. (d) SC mode propagation analysis when a light beam is incident on the PC. Here, $\mathbf{k}_{\text{in},r,t}$ ($\mathbf{v}_{\text{in},r,t}$, $\theta_{\text{in},r,t}$) are the wave vectors (group velocities, angles) of the incident, reflected, and transmitted beams, respectively. (e) Distribution of $E_z(x, y)$ for the SC mode when excited by a Gaussian beam at normal incidence. The small circles show the position of the PC rods.

direction without diffraction. The upper inset illustrates the envelope of the mode intensity along its symmetry axis when the object is either embedded (red and solid lines) or absent (gray and dashed lines). Figure 1(b) shows the detailed geometry and parameters of the system. The square latticed PC is composed of silicon nanorods ($n_a = 3.4$) in water ($n_b = 1.33$), and the radius of the nanorods is $r = 0.1a$, a being the lattice constant of the PC. A cylindrical object of refractive index n_o and semiaxes r_x and r_y is embedded in the lattice, centered on the symmetry axis of the SC mode.

The equifrequency contours of the PC are obtained using the plane wave expansion method [60], as shown in Fig. 1(c) (the second band). At $\omega = 0.5(2\pi c/a)$, the equifrequency contour has a square shape with straight sides, which is the key feature of the SC mode. According to the definition of group velocity $\mathbf{v}_g = \nabla_k \omega(k)$, this SC mode propagates only along the x or y directions.

When a Gaussian beam is incident on the surface of the PC, the excitation of this SC mode can be understood as shown in Fig. 1(d). Its Poynting's vector will always be along the x direction if the angle of θ_{in} is less than the critical angle, which is approximately $\pm 30°$ for the current structure. Figure 1(e) shows the electric field distribution of the SC mode propagating a distance over $100a$, where no diffraction is observed. It should be noted that we have set $x = 0$ at $20a$ inside the PC in order to remove the influence of the lattice surface. In principle, this distance without diffraction is infinite, thus being limited only by the physical length of the structure, which guarantees a long-range pulling.

When the object is illuminated by the SC mode, the time-averaged total optical force can be obtained by integrating the Maxwell's stress tensor on a closed surface surrounding it [61]:

$$\langle \mathbf{F}_{\text{total}} \rangle = \int_S \langle \mathbf{T} \rangle \cdot d\mathbf{s} \quad \text{with}$$
$$\langle \mathbf{T} \rangle = \frac{1}{2}\text{Re}[\mathbf{D} \otimes \mathbf{E}^* + \mathbf{H} \otimes \mathbf{B}^* - \frac{1}{2}\overleftrightarrow{\mathbf{I}}(\mathbf{E} \cdot \mathbf{D}^* + \mathbf{H} \cdot \mathbf{B}^*)]. \tag{1}$$

Here, $\langle \cdot \rangle$ means time average, $\otimes$ stands for dyadic operation, and $\overleftrightarrow{\mathbf{I}}$ is the unit tensor. All electromagnetic fields in Eq. (1) are obtained using the finite-difference time-domain algorithm.

Since the shape of the object plays an important role in the optical force [62–66], we present in Fig. 2 the dependence of the total optical force $F_{x,\text{total}}$ on the central position x_o and the shape of the scatterer. The other

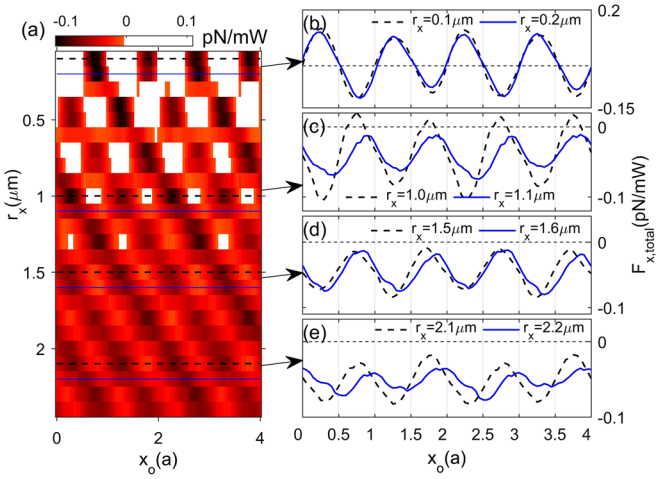

FIG. 2. Illustrating how the total optical force $F_{x,\text{total}}$ changes with the shape of the object. $r_y = 0.1$ μm is fixed, and r_x varies from 0.1 to 2.4 μm. (a) Changes of $F_{x,\text{total}}$ vs (x_o, r_x). The regions with positive forces are in white. (b) Optical force for $r_x = 0.1$ μm (black dashed curve) and $r_x = 0.2$ μm (blue curve). (c)–(e) show the same as (b) except for different r_x.

parameters are $n_o = 1.50$, $r_y = 0.1$ μm, and r_x varies from 0.1 to 2.4 μm. When r_x is small, $F_{x,\text{total}}$ alternates its direction from the positive to negative with period a, as shown in Fig. 2(b). This is easy to understand if we notice that the intensity distribution of the SC mode is periodic also. As r_x increases, however, the negative forces become more and more significant, while their positive components occur only in very narrow regions (around $x = 0.75a$, $1.75a$, etc.), as shown in Fig. 2(c). More intriguingly, $F_{x,\text{total}}$ can be continuously negative for some values of r_x, as shown in Figs. 2(d) and 2(e). This pulling force is unique to the SC mode, which is absent even for the negative refraction frequency of the photonic crystal [67].

Now, we proceed to decompose the total optical force into the gradient and scattering components. This allows us to better understand the nature of the pulling force. For a dipole sphere with radius r, the optical gradient force is [5]

$$\mathbf{F}_{\text{grad}} = \frac{2\pi n_b r^3}{c}\left(\frac{n_o^2/n_b^2 - 1}{n_o^2/n_b^2 + 2}\right)\nabla I(x,y) = V\frac{3n_b}{2c}\left(\frac{n_o^2/n_b^2 - 1}{n_o^2/n_b^2 + 2}\right)\nabla I(x,y) = V \cdot \mathbf{f}_{\text{grad}}. \quad (2)$$

Here $I(x,y) \propto |E(x,y)|^2$ is the light intensity. Since $V = 4\pi r^3/3$ is the volume of the object, $\mathbf{f}_{\text{grad}}$ can be regarded as the gradient force density inside the scatterer. In the current situation, the object is large and cannot be considered as a single dipole. In this situation, according to the concept of the discrete dipole approximation [68,69], we divide the whole object into multiple dipoles and calculate the gradient force $\mathbf{F}_{\text{grad},i}$ of the ith dipole from Eq. (2). Then, the total gradient force can be obtained by the summation of $\mathbf{F}_{\text{grad},i}$ over all these dipoles. In the limit case, the total gradient force can be calculated by volume integration of $\mathbf{f}_{\text{grad}}$ over the object, i.e.,

$$\mathbf{F}_{\text{grad}} = \iiint_{\text{object}} \mathbf{f}_{\text{grad}} dV = \frac{3n_b}{2c}\left(\frac{n_o^2/n_b^2 - 1}{n_o^2/n_b^2 + 2}\right)\iiint_{\text{object}} \nabla I(x,y,z) dV. \quad (3)$$

The results of the calculation following Eq. (3) are shown in Fig. 3(a), which agree well with the total optical force $F_{x,\text{total}}$ calculated by Eq. (1). The small differences between $F_{x,\text{total}}$ and $F_{x,\text{grad.}}$ confirm that the pulling force at $r_x = 1.9$ μm is predominately due to the gradient component (for other cases of r_x, the differences may be slightly larger, but the gradient force is still the dominant component). This is in contrast with the widely held conception that the optical pulling force would be a scattering force [26,27]. Also, this is a surprising result, since so far it was believed in all research work that the intensity gradient force can be used only to trap objects, like in standard optical tweezers, but not, as shown here, for the transportation over a long range.

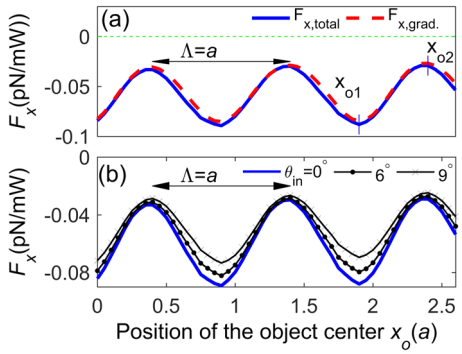

FIG. 3. (a) The solid (blue) curve is the total optical force calculated by Eq. (1), and the dashed (red) curve shows the gradient force calculated by Eq. (3), at normal incidence. The parameters are $r_y = 0.1$ μm and $r_x = 1.9$ μm, and x_{o1} and x_{o2} are two typical positions of the object center that are further analyzed in Fig. 4. (b) Variation of F_x vs the incidence angles of $\theta_{\text{in}} = 0°$, 6°, and 9°.

It is now interesting to explore how the gradient force can result in a continuously optical pulling force over a long range. Figure 4(a) shows the intensity pattern of the SC mode scattered by the object located at x_{o1} [cf. Fig. 3(a)]. The inset shows the details by a zoom around the object, in which the integration path for the force calculation is also shown for reference. In order to clearly observe the active

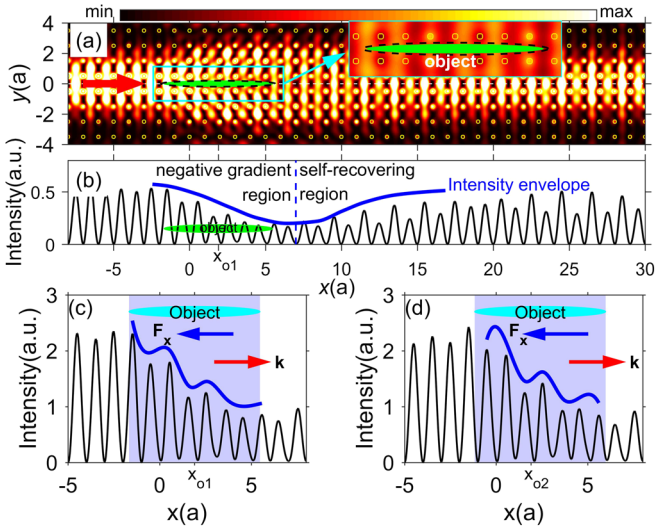

FIG. 4. (a) Self-induced backaction of the object on the SC mode at normal incidence. The inset shows an enlarged image of the object, where the integration path (black and dashed lines) for the force calculation is also shown. The object is centered at $x_{o2} = 1.9a$ [cf. Fig. 3(a)]. All the other parameters are the same as those in Fig. 3(a). (b) Section of (a) along the SC beam axis $y = 0$. The blue curve (solid) shows the SC intensity envelope. Since the object locates in the negative gradient region, it will be pulled by the negative gradient force towards the source. (c) Enlargement of the negative intensity profile of (b) around the object. (d) The same as (c) except for the object centered at $x_{o2} = 2.4a$ [cf. Fig. 3(a)].

backaction of the object on the SC mode, we also plot the cross section of Fig. 4(a) in Fig. 4(b). One can see both in Figs. 4(a) and 4(b) that the backaction of the object significantly modifies the SC mode profile, and the *negative gradient region* and *self-recovering region* are formed. As a result, the left side of the object (around $x \sim 0a$) locates in a higher-intensity region, while the right side ($x \sim 5a$) locates in a much lower-intensity region. Thus, the object experiences a negative intensity gradient and, in turn, a pulling force. Here, it is noted that there is momentum exchange between the SC mode and the PC lattice locally. This can be verified by calculating the force exerted on the lattice atoms in the vicinity of the object.

When the object shifts from x_{o1} to x_{o2}, the intensity envelope *shifts synchronously following the object displacement* [see Figs. 4(c) and 4(d)]; thus, the local gradient pulling of the object is maintained. This is what makes the gradient force continuously negative during the pulling process. This feature is sharply different from those in tractor beams reported before, where the scattering force and the forward momentum enhancement dominate the pulling force. For example, for the interfacial tractor beam proposed in Ref. [38], the gradient force component does not predominate in the total pulling force (see Sec. 1 in Supplemental Material [70] for more details).

Actually, the optical pulling force stemming from the intensity gradient also exists in ordinary optical tweezers. When an object enters the region ahead of the focus of the optical tweezers, it also experiences a negative gradient force towards the focal point. However, the pulling force cannot be maintained once the object arrives at the focus, where the object is trapped; i.e., the potential in the tweezers is achieved by external lenses, which can only pull the object transiently and finally trap it to the focus. By contrast, the intensity gradient force presented here is generated by the object itself rather than by an external system. Thus, the object can also "see" the well, but it can never reach and be trapped there, since it is induced by and moves synchronously with the object. Therefore, it can pull the object continuously and endlessly. In other words, the object in the current situation is not only the entity to be manipulated, but it also acts as a focusing lens that generates the intensity gradient. From this point of view, the object is pulled by the intensity gradient formed by itself. This is the reason that makes the gradient force continuously negative during the long-range pulling process.

From Figs. 4(a) and 4(b), it is observed that the SC mode can recover itself through the self-recovering region (certainly, there is a small scattering loss induced by the object). This feature is similar to the self-healing property of the Bessel beam, though the mechanism is different [71]. This suggests that the tractor beam can manipulate multiple objects simultaneously (see Sec. 2 in Supplemental Material [70] for more details).

The pulling force reported here is not difficult to observe in experiments, because the SC mode is insensitive to frequency detuning, small random deviations in the lattice, and the incident angle of the source. Figure 3(b) displays the pulling forces at different angles $\theta_{\text{in}} = 0°$, 6°, and 9°, and optical pulling is obtained in all these cases. This is understandable, since the SC mode can be excited within a wide range of θ_{in}. However, as θ_{in} increases, the amplitude of the pulling force diminishes due to the decrease of the coupling efficiency at larger θ_{in}. Apart from the pulling force in the x direction, the force in the y direction is found to be a restoring one within the range of $y_o \in [-0.1a, 0.1a]$, which binds the object to the symmetry axis of the SC mode. This means that the pulling manipulation is stable. For experimental observation, one may replace the two-dimensional PC adopted here using more realistic PCs [57,58], where the SC modes have been predicted theoretically and also demonstrated experimentally (see Sec. 3 in Supplemental Material [70] for more details).

The optical pulling operation proposed here exhibits several features different from its conventional counterparts reported before. First, optical tractor beams have been achieved by gradientless optical beams before. By contrast, the current tractor beam's local intensity periodically oscillates. Second, the pulling force is mainly due to the gradient component rather than to the scattering force. Third, the tractor beam based on the SC mode is in standard PCs and can be excited with a single Gaussian beam within a large range of incidence angles. Finally, it is flexibly scalable in the whole spectrum by engineering the periodicity of the PC and can pull multiple scatterers simultaneously. This unique optical pulling force can find broad applications in microfluidic environments, such as an optical conveyor [31,34], which is highly desired in the transportation of small particles. It can also be used as optical sorting, since the force direction varies with the particle size [29,52].

In conclusion, we have put forward a novel optical force in a tailored photonic crystal background which hosts a self-collimating beam to function as an optical tractor beam that can continuously pull one or multiple objects to the source over a long spatial range. Our systematic analyses reveal that the pulling force originates mainly from a new mechanism based on the local intensity gradient induced by the active backaction of the object to the self-collimation mode rather than by a standard scattering force. In addition to this well-distinguished underlying mechanism, this new tractor beam exhibits significant exciting merits. For example, the self-collimation frequency can be easily devised in a photonic crystal lattice as well as efficiently excited using an ordinary Gaussian beam within a wide range of incidence angles. Hence, the concept and results presented in this work provide a novel, insightful, and practically feasible method to tailoring optical forces, leading to more general procedures of optical manipulation.

This work was supported by National Natural Science Foundation of China (Grants No. 11474077 and No. 11404083) and Program for Innovation Research of Science in Harbin Institute of Technology (Grants No. A201411 and No. B201407). M. N.-V.'s work was supported by MINECO-FEDER, Grants No. FIS2014-55563-REDC and No. FIS2015-69295-C3-1-P. C.-W. Q. acknowledges the support from Ministry of Education, Singapore (Grant No. R-263-000-D11-114). We thank the HPC Studio at Physics Department of Harbin Institute of Technology for access to computing resources through INSPUR-HPC@PHY.HIT.

*y.liu@northeastern.edu
†chengwei.qiu@nus.edu.sg
‡wqding@hit.edu.cn

[1] A. Ashkin and J. P. Gordon, Opt. Lett. **8**, 511 (1983).
[2] A. Ashkin, J. M. Dziedzic, J. E. Bjorkholm, and S. Chu, Opt. Lett. **11**, 288 (1986).
[3] A. Ashkin, Phys. Rev. Lett. **24**, 156 (1970).
[4] O. M. Maragò, P. H. Jones, P. G. Gucciardi, G. Volpe, and A. C. Ferrari, Nat. Nanotechnol. **8**, 807 (2013).
[5] K. C. Neuman and S. M. Block, Rev. Sci. Instrum. **75**, 2787 (2004).
[6] J. R. Moffitt, Y. R. Chemla, S. B. Smith, and C. Bustamante, Annu. Rev. Biochem. **77**, 205 (2008).
[7] D. G. Grier, Nature (London) **424**, 810 (2003).
[8] K. Svoboda, Annu. Rev. Biophys. Biomol. Struct. **23**, 247 (1994).
[9] M. Soltani, J. Lin, R. A. Forties, J. T. Inman, S. N. Saraf, R. M. Fulbright, M. Lipson, and M. D. Wang, Nat. Nanotechnol. **9**, 448 (2014).
[10] F. M. Fazal and S. M. Block, Nat. Photonics **5**, 318 (2011).
[11] G. S. Wiederhecker, L. Chen, A. Gondarenko, and M. Lipson, Nature (London) **462**, 633 (2009).
[12] M. Eichenfield, J. Chan, R. M. Camacho, K. J. Vahala, and O. Painter, Nature (London) **462**, 78 (2009).
[13] M. Eichenfield, C. P. Michael, R. Perahia, and O. Painter, Nat. Photonics **1**, 416 (2007).
[14] F. Brennecke, S. Ritter, T. Donner, and T. Esslinge, Science **322**, 235 (2008).
[15] T. P. Purdy, P. L. Yu, R. W. Peterson, N. S. Kampel, and C. A. Regal, Phys. Rev. X **3**, 031012 (2013).
[16] N. Descharmes, U. P. Dharanipathy, Z. Diao, M. Tonin, and R. Houdré, Phys. Rev. Lett. **110**, 123601 (2013).
[17] J. Berthelot, S. S. Acimovic, M. L. Juan, M. P. Kreuzer, J. Renger, and R. Quidant, Nat. Nanotechnol. **9**, 295 (2014).
[18] M. L. Juan, M. Righini, and R. Quidant, Nat. Photonics **5**, 349 (2011).
[19] P. Mestres, J. Berthelot, S. S. Aćimović, and R. Quidant, Light Sci. Appl. **5**, e16092 (2016).
[20] L. Neumeier, R. Quidant, and D. E. Chang, New. J. Phys. **17**, 123008 (2015).
[21] J.-H. Kang, K. Kim, H.-S. Ee, Y.-H. Lee, T.-Y. Yoon, M.-K. Seo, and H.-G. Park, Nat. Commun. **2**, 582 (2011).
[22] A. Kotnala and R. Gordon, Nano Lett. **14**, 853 (2014).
[23] P. L. Marston, J. Acoust. Soc. Am. **120**, 3518 (2006).
[24] P. L. Marston, J. Acoust. Soc. Am. **122**, 3162 (2007).
[25] L. Zhang and P. L. Marston, Phys. Rev. E **84**, 035601(R) (2011).
[26] J. Chen, J. Ng, Z. Lin, and C. T. Chan, Nat. Photonics **5**, 531 (2011).
[27] A. Novitsky, C.-W. Qiu, and H. Wang, Phys. Rev. Lett. **107**, 203601 (2011).
[28] A. Novitsky, C.-W. Qiu, and A. Lavrinenko, Phys. Rev. Lett. **109**, 023902 (2012).
[29] O. Brzobohatý, V. Karásek, M. Šiler, L. Chvátal, T. Čižmár, and P. Zemánek, Nat. Photonics **7**, 123 (2013).
[30] S. Sukhov and A. Dogariu, Opt. Lett. **35**, 3847 (2010).
[31] D. B. Ruffner and D. G. Grier, Phys. Rev. Lett. **109**, 163903 (2012).
[32] S. Sukhov and A. Dogariu, Phys. Rev. Lett. **107**, 203602 (2011).
[33] C. E. M. Démoré, P. M. Dahl, Z. Yang, P. Glynne-Jones, A. Melzer, S. Cochran, M. P. MacDonald, and G. C. Spalding, Phys. Rev. Lett. **112**, 174302 (2014).
[34] V. Intaraprasonk and S. Fan, Opt. Lett. **38**, 3264 (2013).
[35] K. Ding, J. Ng, L. Zhou, and C. T. Chan, Phys. Rev. A **89**, 063825 (2014).
[36] N. Wang, J. Chen, S. Liu, and Z. Lin, Phys. Rev. A **87**, 063812 (2013).
[37] A. Dogariu, S. Sukhov, and J. J. Sáenz, Nat. Photonics **7**, 24 (2013).
[38] V. Kajorndejnukul, W. Ding, S. Sukhov, C.-W. Qiu, and A. Dogariu, Nat. Photonics **7**, 787 (2013).
[39] V. Shvedov, A. R. Davoyan, C. Hnatovsky, N. Engheta, and W. Krolikowski, Nat. Photonics **8**, 846 (2014).
[40] S.-H. Lee, Y. Roichman, and D. G. Grier, Opt. Express **18**, 6988 (2010).
[41] A. Mizrahi and Y. Fainman, Opt. Lett. **35**, 3405 (2010).
[42] K. J. Webb and Shivanand, Phys. Rev. E **84**, 057602 (2011).
[43] M. Nieto-Vesperinas, J. J. Sáenz, R. Gómez-Medina, and L. Chantada, Opt. Express **18**, 11428 (2010).
[44] A. V. Maslov, Phys. Rev. Lett. **112**, 113903 (2014).
[45] A. Salandrino and D. N. Christodoulides, Opt. Lett. **36**, 3103 (2011).
[46] D. E. Fernandes and M. G. Silveirinha, Phys. Rev. A **91**, 061801 (2015).
[47] C. Pfeiffer and A. Grbic, Phys. Rev. B **91**, 115408 (2015).
[48] D. Gao, W. Ding, M. Nieto-Vesperinas, X. Ding, M. Rahman, T. Zhang, C. T. Lim, and C.-W. Qiu, Light Sci. Appl. **6**, e17039 (2017).
[49] J. Lu, H. Yang, L. Zhou, Y. Yang, S. Luo, Q. Li, and M. Qiu, Phys. Rev. Lett. **118**, 043601 (2017).
[50] V. Shvedov, A. R. Davoyan, C. Hnatovsky, N. Engheta, and W. Krolikowski, Nat. Photonics **8**, 846 (2014).
[51] M. Wang, H. Li, D. Gao, L. Gao, J. Xu, and C.-W. Qiu, Opt. Express **23**, 16546 (2015).
[52] T. Zhang, M. R. C. Mahdy, Y. Liu, J. H. Teng, C. T. Lim, Z. Wang, and C.-W. Qiu, ACS Nano **11**, 4292 (2017).
[53] C.-W. Qiu, W. Ding, M. R. C. Mahdy, D. Gao, T. Zhang, F. C. Cheong, A. Dogariu, Z. Wang, and C. T. Lim, Light Sci. Appl. **4**, e278 (2015).
[54] T. Zhu, A. Novitsky, Y. Cao, M. R. C. Mahdy, L. Wang, F. Sun, Z. Jiang, and W. Ding, Appl. Phys. Lett. **111**, 061105 (2017).
[55] E. Yablonovitch, Phys. Rev. Lett. **58**, 2059 (1987).
[56] S. John, Phys. Rev. Lett. **58**, 2486 (1987).

[57] H. Kosaka, T. Kawashima, A. Tomita, M. Notomi, T. Tamamura, T. Sato, and S. Kawakami, Appl. Phys. Lett. **74**, 1212 (1999).
[58] H. Kosaka, T. Kawashima, A. Tomita, M. Notomi, T. Tamamura, T. Sato, and S. Kawakami, Phys. Rev. B **58**, R10096 (1998).
[59] C. Luo, S. G. Johnson, J. D. Joannopoulos, and J. B. Pendry, Phys. Rev. B **65**, 201104(R) (2002).
[60] S. G. Johnson and J. D. Joannopoulos, Opt. Express **8**, 173 (2001).
[61] J. D. Jackson, *Classical Electrodynamics*, 3rd ed. (Wiley, New York, 1998).
[62] S. H. Simpson, S. Hanna, T. J. Peterson, and G. A. Swartzlander, Opt. Lett. **37**, 4038 (2012).
[63] G. A. Swartzlander, Jr, T. J. Peterson, A. B. Artusio-Glimpse, and A. D. Raisanen, Nat. Photonics **5**, 48 (2011).
[64] D. B. Phillips, M. J. Padgett, S. Hanna, Y. L. D. Ho, D. M. Carberry, M. J. Miles, and S. H. Simpson, Nat. Photonics **8**, 400 (2014).
[65] A. B. Artusio-Glimpse, T. J. Peterson, and G. A. Swartzlander, Opt. Lett. **38**, 935 (2013).
[66] A. B. Artusio-Glimpse, D. G. Schuster, M. W. Gomes, and G. A. Swartzlander, Appl. Opt. **53**, I1 (2014).
[67] A. S. Ang, S. V. Sukhov, A. Dogariu, and A. S. Shalin, Sci. Rep. **7**, 41014 (2017).
[68] L. Ling, F. Zhou, L. Huang, and Z.-Y. Li, J. Appl. Phys. **108**, 073110 (2010).
[69] B. T. Draine and P. J. Flatau, J. Opt. Soc. Am. A **11**, 1491 (1994).
[70] See Supplemental Material at http://link.aps.org/supplemental/10.1103/PhysRevLett.120.123901 for more detailed simulation results about the features of the optical pulling force.
[71] J. Arlt and K. Dholakia, Opt. Commun. **177**, 297 (2000).

Correction: A second affiliation was inserted for the first author.